Enhanced coherence between condensates formed resonantly at different times.

Alex Hayat,[1,*] Christoph Lange,[2] Lee A. Rozema,[2] Rockson Chang,[2] Shreyas Potnis,[2] Henry M. van Driel,[2] Aephraim M. Steinberg,[2,3] Mark Steger,[4] David W. Snoke,[4] Loren N. Pfeiffer[5] and Kenneth W. West[5]

[1]*Department of Electrical Engineering, Technion, Haifa 32000, Israel*
[2]*Department of Physics, Centre for Quantum Information and Quantum Control, and Institute for Optical Sciences, University of Toronto, Toronto, Ontario M5S 1A7, Canada*
[3]*Canadian Institute for Advanced Research, Toronto, Ontario M5G 1Z8, Canada*
[4]*Dept. of Physics and Astronomy, University of Pittsburgh, Pittsburgh, PA 15260, USA*
[5]*Dept. of Electrical Engineering, Princeton University, Princeton, N J 08544, USA*
[*]*alex.hayat@ee.technion.ac.il*

Abstract: We demonstrate coherence between exciton-polariton condensates created resonantly at different times. The coherence persists much longer than the individual particle dephasing time, and this persistence increases as the particle density increases. The observed coherence time exceeds that of the injecting laser pulse by more than an order of magnitude. We show that this significant coherence enhancement relies critically on the many-body particle interactions, as verified by its dependence on particle density, interaction strength, and bath temperature, whereas the mass of the particles plays no role in the condensation of resonantly injected polaritons. Furthermore, we observe a large nonlinear phase shift resulting from intra-condensate interaction energy. Our results provide a new approach for probing ultrafast dynamics of resonantly-created condensates and open new directions in the study of coherence in matter.

OCIS codes: (020.1475) Bose-Einstein condensates; (320.7130) Ultrafast processes in condensed matter, including semiconductors ; (140.3945) Microcavities; (190.4390) Nonlinear optics, integrated optics.

References and links:

1. M. H. Anderson, J. R. Ensher, M. R. Matthews, C. E. Wieman, and E. A. Cornell, "Observation of Bose-Einstein condensation in a dilute atomic vapor," Science **269**(5221), 198–201 (1995).
2. K. B. Davis, M.-O. Mewes, M. R. Andrews, D. S. Durfee, D. M. Kurn, and W. Ketterle, "Bose-Einstein condensation in a gas of sodium atoms," Phys. Rev. Lett. **75**(22), 3969–3973 (1995).
3. J. Kasprzak, M. Richard, S. Kundermann, A. Baas, P. Jeambrun, J. M. J. Keeling, F. M. Marchetti, M. H. Szymańska, R. André, J. L. Staehli, V. Savona, P. B. Littlewood, B. Deveaud, and S. Dang, "Bose-Einstein condensation of exciton polaritons," Nature **443**(7110), 409–414 (2006).
4. H. Deng, G. Weihs, C. Santori, J. Bloch, and Y. Yamamoto, "Condensation of semiconductor microcavity exciton polaritons," Science **298**(5591), 199–202 (2002).
5. R. Balili, V. Hartwell, D. Snoke, L. Pfeiffer, and K. West, "Bose-Einstein condensation of microcavity polaritons in a trap," Science **316**(5827), 1007–1010 (2007).
6. Y. Shin, M. Saba, T. A. Pasquini, W. Ketterle, D. E. Pritchard, and A. E. Leanhardt, "Atom interferometry with Bose-Einstein condensates in a double-well potential," Phys. Rev. Lett. **92**(5), 050405 (2004).
7. T. Schumm, S. Hofferberth, L. M. Andersson, S. Wildermuth, S. Groth, I. Bar-Joseph, J. Schmiedmayer, and P. Krüger, "Matter-wave interferometry in a double well on an atom chip," Nat. Phys. **1**(1), 57–62 (2005).
8. E. Wertz, L. Ferrier, D. D. Solnyshkov, R. Johne, D. Sanvitto, A. Lemaître, I. Sagnes, R. Grousson, A. V. Kavokin, P. Senellart, G. Malpuech, and J. Bloch, "Spontaneous formation and optical manipulation of extended polariton condensates," Nat. Phys. **6**(11), 860–864 (2010).
9. G. Tosi, G. Christmann, N. G. Berloff, P. Tsotsis, T. Gao, Z. Hatzopoulos, P. G. Savvidis, and J. J. Baumberg, "Sculpting oscillators with light within a nonlinear quantum fluid," Nat. Phys. **8**(3), 190–194 (2012).
10. N. Krizhanovskii, K. G. Lagoudakis, M. Wouters, B. Pietka, R. A. Bradley, K. Guda, D. M. Whittaker, M. S. Skolnick, B. Deveaud-Plédran, M. Richard, R. André, and L. Dang, "Coexisting nonequilibrium condensates with long-range spatial coherence in semiconductor microcavities," Phys. Rev. B **80**(4), 045317 (2009).

#224691 - $15.00 USD Received 9 Oct 2014; revised 18 Nov 2014; accepted 19 Nov 2014; published 1 Dec 2014

11. A. J. Leggett, *Quantum Liquids: Bose Condensation and Cooper Pairing in Condensed Matter Systems* (Oxford University Press, 2006).
12. C. Weisbuch, M. Nishioka, A. Ishikawa, and Y. Arakawa, "Observation of the coupled exciton-photon mode splitting in a semiconductor quantum microcavity," Phys. Rev. Lett. **69**(23), 3314–3317 (1992).
13. D. Sanvitto, S. Pigeon, A. Amo, D. Ballarini, M. De Giorgi, I. Carusotto, R. Hivet, F. Pisanello, V. G. Sala, P. S. S. Guimaraes, R. Houdré, E. Giacobino, C. Ciuti, A. Bramati, and G. Gigli, "All-optical control of the quantum flow of a polariton condensate," Nat. Photonics **5**(10), 610–614 (2011).
14. A. Amo, S. Pigeon, D. Sanvitto, V. G. Sala, R. Hivet, I. Carusotto, F. Pisanello, G. Leménager, R. Houdré, E. Giacobino, C. Ciuti, and A. Bramati, "Polariton superfluids reveal quantum hydrodynamic solitons," Science **332**(6034), 1167–1170 (2011).
15. A. Amo, D. Sanvitto, F. P. Laussy, D. Ballarini, E. del Valle, M. D. Martin, A. Lemaître, J. Bloch, D. N. Krizhanovskii, M. S. Skolnick, C. Tejedor, and L. Viña, "Collective fluid dynamics of a polariton condensate in a semiconductor microcavity," Nature **457**(7227), 291–295 (2009).
16. D. Sanvitto, F. M. Marchetti, M. H. Szymańska, G. Tosi, M. Baudisch, F. P. Laussy, D. N. Krizhanovskii, M. S. Skolnick, L. Marrucci, A. Lemaître, J. Bloch, C. Tejedor, and L. Viña, "Persistent currents and quantized vortices in a polariton superfluid," Nat. Phys. **6**(7), 527–533 (2010).
17. K. G. Lagoudakis, M. Wouters, M. Richard, A. Baas, I. Carusotto, R. André, L. S. Dang, and B. Deveaud-Plédran, "Quantized vortices in an exciton–polariton condensate," Nat. Phys. **4**(9), 706–710 (2008).
18. R. Spano, J. Cuadra, C. Lingg, D. Sanvitto, M. D. Martin, P. R. Eastham, M. van der Poel, J. M. Hvam, and L. Viña, "Build up of off-diagonal long-range order in microcavity exciton-polaritons across the parametric threshold," Opt. Express **21**(9), 10792–10800 (2013).
19. V. E. Hartwell and D. W. Snoke, "Numerical simulations of the polariton kinetic energy distribution in GaAs quantum-well microcavity structures," Phys. Rev. B **82**(7), 075307 (2010).
20. A. Hayat, C. Lange, L. A. Rozema, A. Darabi, H. M. van Driel, A. M. Steinberg, B. Nelsen, D. W. Snoke, L. N. Pfeiffer, and K. W. West, "Dynamic Stark Effect in Strongly Coupled Microcavity Exciton Polaritons," Phys. Rev. Lett. **109**(3), 033605 (2012).
M. Steger, C. Gautham, B. Nelsen, D. Snoke, L. Pfeiffer, and K. West, "Single-wavelength, all-optical switching based on exciton-polaritons," Appl. Phys. Lett. **101**(13), 131104 (2012).
21. B. Fluegel, N. Peyghambarian, G. Olbright, M. Lindberg, S. W. Koch, M. Joffre, D. Hulin, A. Migus, and A. Antonetti, "Femtosecond studies of coherent transients in semiconductors," Phys. Rev. Lett. **59**(22), 2588–2591 (1987).
22. M. Assmann, J. S. Tempel, F. Veit, M. Bayer, A. Rahimi-Iman, A. Löffler, S. Höfling, S. Reitzenstein, L. Worschech, and A. Forchel, "From polariton condensates to highly photonic quantum degenerate states of bosonic matter," Proc. Natl. Acad. Sci. U.S.A. **108**(5), 1804–1809 (2011).
23. S. Utsunomiya, L. Tian, G. Roumpos, C. W. Lai, N. Kumada, T. Fujisawa, M. Kuwata-Gonokami, A. Löffler, S. Höfling, A. Forchel, and Y. Yamamoto, "Observation of Bogoliubov excitations in exciton-polariton condensates," Nat. Phys. **4**(9), 700–705 (2008).
24. C. J. Pethick and H. Smith, *Bose-Einstein Condensation in Dilute Gases* (Cambridge university press. 2001).
25. M. Wouters and I. Carusotto, "Excitations in a nonequilibrium Bose-Einstein condensate of exciton polaritons," Phys. Rev. Lett. **99**(14), 140402 (2007).
26. E. Wertz, L. Ferrier, D. D. Solnyshkov, P. Senellart, D. Bajoni, A. Miard, A. Lemaître, G. Malpuech, and J. Bloch, "Spontaneous formation of a polariton condensate in a planar GaAs microcavity," Appl. Phys. Lett. **95**(5), 051108 (2009).
27. J. S. Tempel, F. Veit, M. Aßmann, L. E. Kreilkamp, S. Höfling, M. Kamp, A. Forchel, and M. Bayer, "Temperature dependence of pulsed polariton lasing in a GaAs microcavity," New J. Phys. **14**(8), 083014 (2012).
28. H.-Y. Lo, Y.-C. Chen, P.-C. Su, H.-C. Chen, J.-X. Chen, Y.-C. Chen, I. A. Yu, and Y.-F. Chen, "Electromagnetically-induced-transparency-based cross-phase-modulation at attojoule levels," Phys. Rev. A **83**(4), 041804 (2011).
29. K. Nemoto and W. J. Munro, "Nearly deterministic linear optical controlled-NOT gate," Phys. Rev. Lett. **93**(25), 250502 (2004).

1. Introduction

Interacting bosons can form coherent states of matter by generating quantum condensates [1–5]. Spatial interferometry has been crucial for the demonstration of macroscopic coherence in cold-atom condensates [6,7] and in the rapidly-developing field of exciton-polariton condensates [8–10]. Such measurements have been performed on steady-state systems, and were therefore unable to access the non-equilibrium dynamics of coherence. Coherence is one of the key properties of quantum condensates [1–5] and superfluids [11], and has been widely studied in various steady-state systems [6–9]. Exciton-polaritons, which emerge from strong light-matter coupling in semiconductor microcavities [12], exhibit a combination of extremely low effective mass and strong polariton-polariton interactions, leading to a wide range of physical phenomena including high-temperature condensation [3–5] and superfluidity [13–17]. A unique advantage of exciton-polariton condensates is that they can be directly accessed

#224691 - $15.00 USD Received 9 Oct 2014; revised 18 Nov 2014; accepted 19 Nov 2014; published 1 Dec 2014

with light, so that various properties such as spin, energy, momentum and phase of the excitation photons are mapped onto polaritons. This attribute has been employed in resonant imprinting of coherence on resonantly-created polariton condensates to generate quantized vortices [16] and to demonstrate long temporal coherence in steady-state condensates using narrowband continuous-wave lasers [18].

Here we demonstrate coherence between two condensates generated resonantly at different times with temporal separation an order of magnitude larger than both the individual particle dephasing time T_2 and the injection laser coherence time. The polariton populations are injected by ultrafast laser pulses which impart an initial coherence to these resonantly-injected populations, but at low particle density this initial coherence is quickly lost. In our pulsed resonantly-excited scheme, stimulated polariton-polariton scattering [19] results in increased decay time of coherence, T_{2c}, which in turn implies spectral narrowing. The polariton populations are injected with different transverse momenta, leading to interference patterns which directly indicate the cross-coherence of the populations. We study the dynamics of coherence by monitoring the interference fringe visibility of the two condensates as a function of temporal separation. At high polariton densities, the coherence between the two resonantly-formed condensates persists for more than an order of magnitude longer than what would be expected from the initially imprinted coherence, so that $T_{2c}>>T_2$. We show that for exciton-like polaritons, the stronger interaction results in larger condensate fraction and thus in longer decay time of coherence – much longer than T_2. Photon-like polaritons, on the other hand, result in lower stimulated scattering rates and thus in generation of a smaller condensate fraction.

2. Experiments and results

In resonant polariton injection, a finite energy range is populated by polaritons with the initial bandwidth determined by the laser and the polariton linewidth. Without polariton condensation the coherence time is limited by the polariton dephasing time, T_2. We have measured this dephasing time in our samples directly to be $T_2< 1$ ps using ultrafast pump-probe spectroscopy [20], by observing the decay of the coherent oscillations [21] [Fig. 1(a)]. The lower polariton (LP) linewidth of ~2 meV observed in reflectance spectra measurements [Fig. 1(d)], is the energy bandwidth of the injected polariton population in our experiment. In the pump-probe differential reflectance spectroscopy experiments, the polarization of the polaritons is nearly instantaneously excited by the short white-light probe pulse and decays exponentially afterwards, leading to an asymmetrical temporal shape of the polarization, which is reasonably well described by $P(t) \sim \Theta(t) e^{-t/T_2} e^{-i\omega t}$ where $\Theta(t)$ is the Heaviside step function, T_2 is the dephasing time, and ω is the polariton frequency. The Fourier-transform of this temporal shape is a Lorentzian, and the FWHM of this Lorentzian is related to T_2 via $T_2 = 2\hbar/\Delta E$, where ΔE is the polariton linewidth. For ΔE ~2meV, the corresponding T_2 ~660 fs. In order to determine the coherence times, we do not rely on the above idealized relation alone. Instead, we perform pump-probe measurements in which the polaritons are first excited by a short white-light pulse. The subsequently freely decaying polarization is then perturbed by a strong, red-detuned pump pulse after a delay time $-\tau_p$.

#224691 - $15.00 USD Received 9 Oct 2014; revised 18 Nov 2014; accepted 19 Nov 2014; published 1 Dec 2014

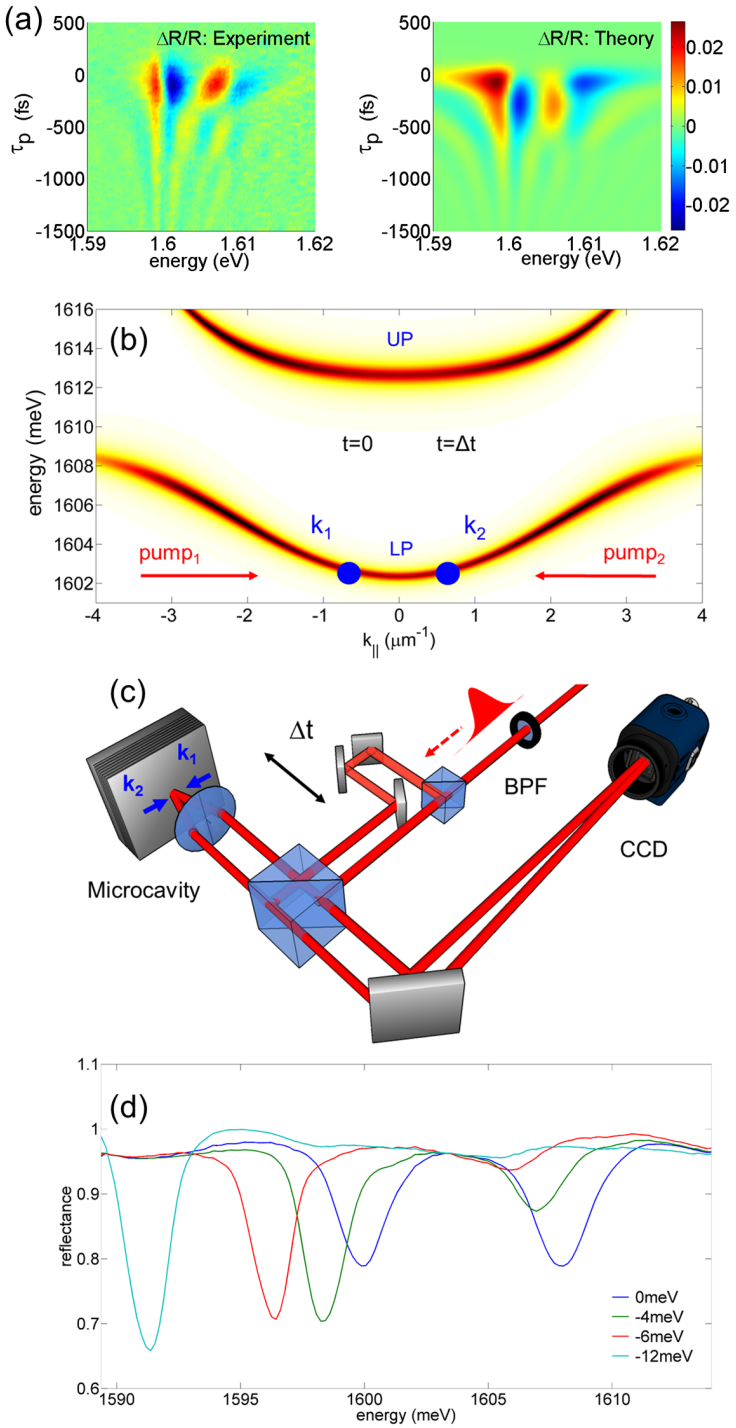

Fig. 1. Time-dependent polariton experiments. (a) Polariton dephasing time, T_2 measurements: differential reflectance ΔR/R spectra in ultrafast pump-probe spectroscopy at 10K temperature and zero detuning measured (left) and calculated (right). $T_2 < 1$ ps is observed in the decay of the coherent oscillations. (b) LP and UP calculated dispersions with a schematic representation of the resonant excitation at different inplane momenta, k_1 and k_2, and at different times $t = 0$ and $t = \Delta t$. (c) Schematic diagram of the experimental setup. (d) Measured reflectance from the sample for various detuning values ΔE.

#224691 - $15.00 USD Received 9 Oct 2014; revised 18 Nov 2014; accepted 19 Nov 2014; published 1 Dec 2014

The effect of the pump is an instantaneous blue-shift of the polariton resonances, which leads to a phase shift of the polarization which accumulates during the pump, and which leads to spectro-temporal oscillations in the reflected intensity. The latter are often referred to as "coherent oscillations" or "perturbed free induction decay". At negative τ_p, the perturbed free induction decay is observed [Fig. 1(a) left panel]. We have thus calculated the response of this experimental setting according to coherent-oscillation theory [21] and adjusted the polarization dephasing time T_2 for best agreement with the experiment. The resulting graph is plotted on [Fig. 1(a) right panel]. The response of one polariton branch selectively can be switched-on in the calculation to remove the interference and obtain the T_2 time of the other branch by fitting an exponential. We obtain T_2 ~550 fs for the LP, and T_2 ~290 fs for the UP.

Therefore, without condensation, the interference visibility must decay rapidly within $T_2 <$ 1 ps. At sufficiently high densities of injected carriers, we observe narrowing of the bandwidth and an interference fringe visibility time well above 10 ps. Thus in the condensed case coherence can be observed between condensates formed at times separated by much longer than T_2, and than the laser coherence time.

Our experiments were performed in a He-flow microscopy cryostat, on a strongly-coupled AlGaAs microcavity grown by molecular beam epitaxy, which consists of a 3λ/2 layer between a bottom 20-layer-pair $Ga_{0.8}Al_{0.2}$/AlAs distributed Bragg reflector (DBR), and a top 16-pair DBR. Single GaAs quantum wells (QW) were placed at each of the 3 antinodes of the microcavity and separated by AlAs barriers. Our structure is similar to the one used in [20]. The thickness of the layers was tapered across the sample to allow tuning of the cavity resonance across the exciton resonance by probing at different locations on the sample.

For initial and final polariton momenta, k_i, k_j, and k_l, k_m, the polariton-polariton scattering matrix element is given by [19] $M \propto \sum_{k_i,k_m} \left(X_{k_i} X_{k_j} X_{k_l} X_{k_m} \right) \Big/ \left| k_i - k_m \right|$. The detuning $\Delta E\left(k_{\|}\right) = E_C\left(k_{\|}\right) - E_X\left(k_{\|}\right)$ of the cavity energy $E_C\left(k_{\|}\right)$ from the exciton energy $E_X\left(k_{\|}\right)$, can be controlled by changing the excitation location due to the tapered layer thickness across the sample. This detuning determines the polariton Hopfield coefficient for the exciton fraction $\left|X_{k_{\|}}\right|^2 = \frac{1}{2}\left(1 + \Delta E\left(k_{\|}\right) \Big/ \sqrt{\Delta E\left(k_{\|}\right)^2 + \left(\hbar\Omega_0\right)^2}\right)$ of the LP, where Ω_0 is the Rabi frequency of exciton-photon coupling. Experimentally, $\Delta E\left(k_{\|}\right)$ was determined by reflection spectroscopy from the sample. The linewidth of the LP remains almost unchanged for the negative detunings in our experiments [Fig. 1(d)].

The output of the ~775 nm, 81 MHz repetition rate Ti:sapphire mode-locked laser was spectrally filtered with a narrow band pass filter (BPF), slightly broader than the polariton linewidth, to result in pulses with ~700 fs coherence time. This coherence time was measured by the interference in our setup on a reflecting sample. The pulse train was split into two paths with a controllable relative time delay, Δt, and recombined on the sample at different angles [Fig. 1(b)] and [Fig. 1(c)]. The measurements were performed for delays longer than 1ps to avoid interference of the excitation pulses. The central wavelength of the pulses was tuned by tilting the BPF, and the incidence angles determined the injected polariton in-plane momenta, k_1 and k_2. Each pulse from the pair injected a polariton population centered at an in-plane momentum given by the excitation pulse angle, and the interference between the two generated condensates formed an interference fringe pattern. Changing the laser wavelength from the polariton resonance reduced the overlap of the laser bandwidth with the polariton line, reducing the condensate fraction and thus the visibility of the interference. The luminescence from the polariton decay in the condensate was imaged onto a charge coupled device (CCD) camera to record the condensate interference pattern. The visibility measurement is averaged over the duration of both condensate lifetimes, T_1. Assuming that the sizes of both condensates are equal, the instantaneous intensity on the CCD is

#224691 - $15.00 USD Received 9 Oct 2014; revised 18 Nov 2014; accepted 19 Nov 2014; published 1 Dec 2014

$$I_t(t) = I(t) + I(t-\Delta t) + 2\sqrt{I(t)I(t-\Delta t)}\cos(2kx)e^{-\Delta t/T_{2c}} + noise \quad (1)$$

Where *I(t)* is the intensity corresponding to each individual condensate alone, T_{2c} is the condensate coherence time, Δt is the delay between the two injection times, and cos(2*kx*) is the spatial interference fringe pattern. The normalized instantaneous visibility at time *t* is then

$$V(t,\Delta t) = \frac{2\sqrt{I(t)I(t-\Delta t)}}{I(t)+I(t-\Delta t)+noise}e^{-\Delta t/T_{2c}} \quad (2)$$

The CCD records the time-integrated intensity $\int I_t(t)\,dt$, so that the extracted visibility is an integral of normalized instantaneous visibility weighted by the instantaneous intensity, while this intensity decays according to the polariton lifetime T_1. For small condensate fraction and thus short T_{2c}, the longer T_1 has almost no effect on the measured visibility ($T_{2c} << T_1$). This short T_{2c} is determined mainly by single-particle dephasing via intra-band scattering which is typically much faster than the inter-band transitions defining T_1. On the other hand, for larger condensate fraction and thus longer T_{2c}, T_1 has a significant effect on the visibility decay time, and the measured T_{2c} can approach T_1.

The first set of interference measurements was performed at a temperature of 10 K with high peak intensity of excitation (corresponding to average intensity of ~10 mWcm^{-2}), with a spot size of approximately 100 μm, and close to zero-detuning cavity-exciton coupling, where both lower LP and UP have nearly equal exciton fractions. The LP was excited resonantly at time $t = 0$, forming a dynamic condensate at an in-plane momentum $k_1 \approx$-0.7 μm^{-1}. At a time $t = \Delta t$, much longer than polariton dephasing time T_2 and the laser coherence time, another population was injected resonantly at an in-plane momentum $k_2 \approx +0.7$ μm^{-1}. The in-plane momentum was chosen to be small enough ($k_1 \approx$-0.7 μm^{-1}) for the spatial interference fringes to be clearly resolved by the imaging system. The two formed condensates have substantial spatial overlap, resulting in a spatial interference pattern [Fig. 2]. This interference, at delay times much longer than polariton dephasing time and the laser coherence time, is a signature of enhanced coherence between the two condensates. Spatial interference in polariton condensates has been employed recently to demonstrate coherence [8,9]. However, our experiments study the interference of two distinct condensates, where initially only one condensate exists, while the second one is formed only at a later time. Moreover, we show the dynamics of condensate formation using pulsed excitation in the cross-coherence between two condensates generated at times separated by longer than T_2, and the laser coherence time.

The LP T_2 at zero detuning in our sample is shorter than 1 ps. For LP condensates in our experiments, the observed coherence persists for longer than T_{2c}~10 ps [Fig. 3(a)]. We performed a similar experiment on two polariton populations in the UP branch. The UP enhanced coherence time was measured to be T_{2c} ~3 ps, which is longer than T_2 ~1 ps, but shorter than T_{2c} of the LP [Fig. 2 UP]. Some polariton population may be redistributed due to scattering over the $|k_{||}| = 0.7$ μm^{-1} ring during the polariton population lifetime in our pulsed experiments. However most of the population in the several ps of the pulse remains at the injected momentum, as can be seen in the interference patterns with clearly oriented interference fringes [Fig. 2]. The LP and UP resonant excitation was achieved by tuning the central wavelength by tilting the dielectric band-pass filter, which slightly affects the spatial profile of the field distribution. The polariton populations in our experiments were injected resonantly into either the LP or the UP branches. The bandwidth of the excitation pulses was much smaller than the energy difference between LP and UP. Therefore LP and UP data were differentiated by the resonant excitation energy.

The long decay time of coherence T_{2c} observed here originates from an emitter with less than a tenth of the initially injected bandwidth. This spectral narrowing results from dynamic

#224691 - $15.00 USD Received 9 Oct 2014; revised 18 Nov 2014; accepted 19 Nov 2014; published 1 Dec 2014

condensation of polaritons and becomes more significant at higher excitation intensities. The shorter coherence time in the UP branch relative to that of the LP is attributed to the faster population decay (e.g. to the LP branch).

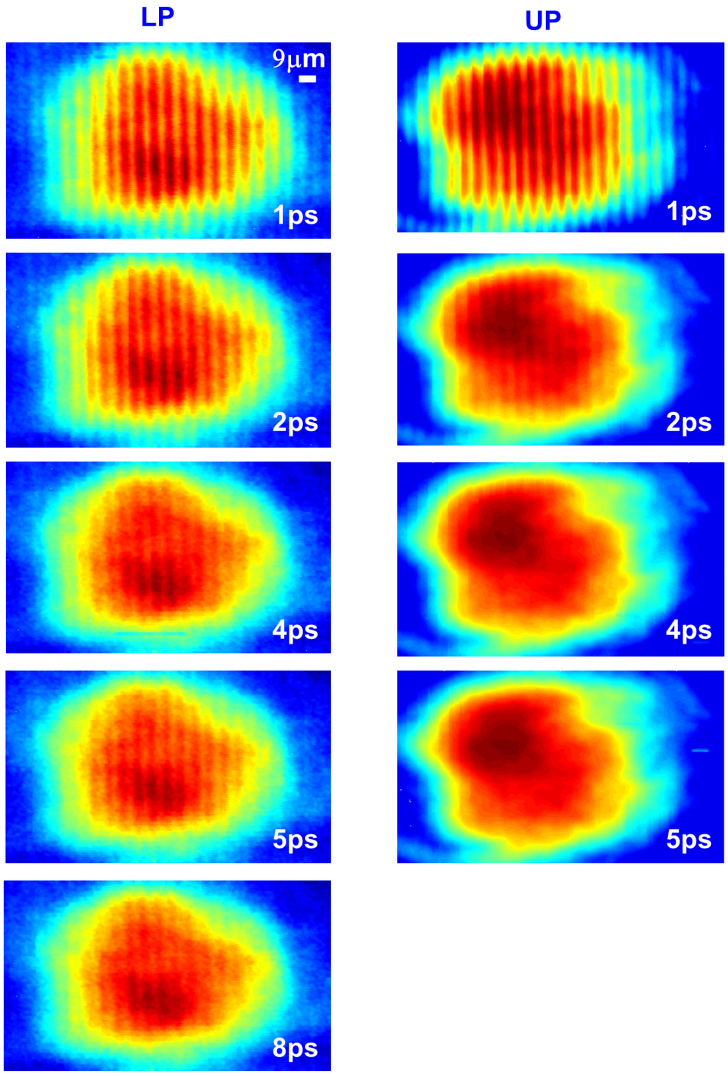

Fig. 2. Interference pattern for different delay times. LP resonant excitation and UP resonant excitation. The average excitation intensity is ~10 mWcm^{-2} – well above the threshold.

Condensate formation results from bosonic stimulated scattering, and in polariton condensation, polariton-polariton scattering has been shown to be the dominant mechanism [22]. The rate of polariton-polariton scattering depends strongly on the excitonic fraction, $\left|X_{k_{\|}}\right|^2$, of the polaritons. Therefore a smaller excitonic Hopfield coefficient, $X_{k_{\|}}$, leads to a smaller condensate fraction. Smaller $X_{k_{\|}}$ also results in shorter lifetime of the polaritons, T_1, which also affects the visibility decay in our pulsed experiments.

#224691 - $15.00 USD Received 9 Oct 2014; revised 18 Nov 2014; accepted 19 Nov 2014; published 1 Dec 2014

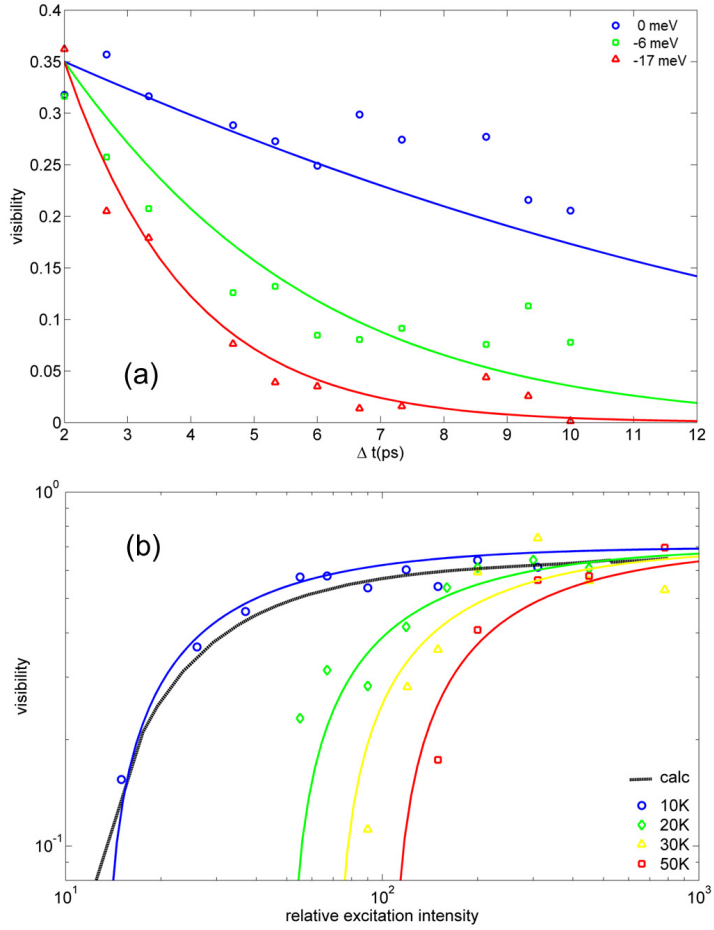

Fig. 3. Coherence measurements. (a) fringe visibility as a function of delay time for various cavity-exciton detunings. The solid lines are the calculated dependence. (b) fringe visibility as a function of excitation intensity for various lattice temperatures and for $\Delta t = 6$ ps. The solid lines are power-law fits as a guide to the eye. The black line is the calculated dependence for T = 0 K, with the maximum visibility as a fitting parameter.

We measured the decay of condensate coherence for several different excitonic fractions of the LP. This was achieved experimentally by controlling the cavity-exciton detuning, ΔE, which changes continuously across the sample. Figure 1(d) shows that the spectral width of the polariton mode changes very little at the detunings used in our experiments, and therefore the number of polaritons created for the three different detunings should be similar. The coherence times T_{2c} were extracted from the calculated curves in Fig. 3 based on Eq. (2). Close to the zero cavity-exciton detuning, (ΔE ≈0), the coherence between the two condensates persists for longer than 10 ps indicating a large condensate fraction [Fig. 3(a)], and the visibility decay is limited only by the condensate lifetime, T_1 – much longer than polariton dephasing, T_2. For a slightly red-detuned cavity (ΔE = −6 meV), the LP is more photon-like, with a smaller excitonic coefficient $X_{k_\parallel}$ resulting in shorter condensate lifetime, T_1, and lower polariton-polariton scattering rate. The lower scattering rate leads to a smaller condensate fraction, which manifests itself in shorter coherence times. An even larger red-detuning of the cavity from the exciton (ΔE = −17 meV) yields an even smaller condensate fraction and shorter coherence times, approaching the limit of photon-like polaritons with no condensation. However, for large excitonic fraction, the fact that the measured visibility decay

#224691 - $15.00 USD Received 9 Oct 2014; revised 18 Nov 2014; accepted 19 Nov 2014; published 1 Dec 2014

time is significantly longer than T_2 and the laser coherence time, is clear evidence of condensation. Larger excitonic fraction may also result in stronger depletion of the condensate [23]. Nevertheless, our data shows that despite the possible depletion, the condensate fraction is larger for larger excitonic fractions. For the bandwidth injected by the laser, without condensation and bandwidth narrowing, the interference visibility must decay as fast as 1ps – even for very long polariton lifetimes. For large excitonic fractions, our measurements show coherence times longer by an order of magnitude than that determined by the injected bandwidth. The shortest possible polariton T_1 occurs for very negative detunings (photon-like polaritons) and is similar to the cavity photon lifetime and photon coherence time < 1ps. This is also similar to the injected polariton bandwidth, which determines the decay time of interference visibility – even for much longer polariton lifetimes T_1. For smaller negative detunings, polariton lifetimes become longer, however this cannot make the decay time of interference visibility longer (without line narrowing and condensation) – regardless of how fast the T_1 increases with detuning. For a short (<1ps) visibility decay time, determined by the injected bandwidth, to become longer (even for very long T_1), the condensate fraction must increase resulting in line narrowing.

In addition to decreasing the polariton scattering rates and T_1, the smaller excitonic fraction results in a smaller LP effective mass $m_{LP} = \left(\left| X_{k_\parallel} \right|^2 / m_X + \left(1 - \left| X_{k_\parallel} \right|^2 \right) / m_C \right)^{-1}$, where m_X and m_C are the exciton and the cavity-photon effective masses, respectively. In equilibrium (or quasi-equilibrium) condensates, smaller mass leads to higher condensate fractions, since the coherence length of the particle wavefunctions (thermal wavelength) must be longer than roughly the inter-particle spacing for condensation to occur [24]. In highly non-equilibrium condensates, formed from resonantly injected polaritons, such as the ones in our experiments, however, the effective mass does not affect the polariton coherence length. The LP coherence is determined directly by the injected momentum bandwidth, and condensation onset depends mainly on the injected polariton density and on the polariton-polariton scattering rate.

In our theoretical modelling, the pump pulse excites a population of polaritons – the reservoir, n_R, over an energy bandwidth that corresponds to the injected optical bandwidth given by T_2. The calculation of condensate coherence dynamics [Fig. 3], as well as the nonlinear phase shift [Fig. 4], were performed using the generalized Gross-Pitaevskii nonlinear equation [25]

$$i\frac{\partial \Psi}{\partial t} = \left[-\frac{\hbar \nabla^2}{2m_{LP}} + \frac{i\left[R(n_R) - \gamma \right]}{2} + g\left|\Psi\right|^2 + g_R n_R \right] \Psi \qquad (3)$$

Where $\gamma = 1/T_1$ is the polariton loss rate. The polariton-polariton interaction within the condensate is modelled by a mean-field coupling constant, g, while the interaction with the polariton reservoir density given by a coupling constant g_R. The dynamics of the polariton reservoir are described by

$$\partial n_R / \partial t = -\gamma n_R - R(n_R)\left|\Psi\right|^2 - D\nabla^2 n_R \qquad (4)$$

where D is the reservoir polariton diffusion constant and $R(n_R)$ is the scattering rate of polaritons from the reservoir into the condensate. The coupled Eqs. (3) and (4) account for stimulated scattering between the polariton reservoir and condensate.

Using the model we have access to the coherent and incoherent populations and we can extract an interference amplitude for comparison with our time-integrated measurements. With simulation parameters scaled within an order of magnitude of the typical values, the calculated dependence of the condensate coherence agrees well with the measurements [Fig.

#224691 - $15.00 USD Received 9 Oct 2014; revised 18 Nov 2014; accepted 19 Nov 2014; published 1 Dec 2014

3]. The simulation parameters are common through each data set (versus detuning), and not retuned for each one.

In order to demonstrate the dependence of the condensate fraction on the polariton density, we studied the dependence of coherence on the excitation intensity. Holding $X_{k_\parallel}$ fixed, increasing the pump intensity should result in a larger condensate fraction, and thus higher coherence at a given delay time of $\Delta t = 6$ ps between two generated condensates. At very low pump powers, the measured coherence is equal to the polariton dephasing time T_2. Our intensity-dependent condensate interference visibility verifies this property [Fig. 3(b)]. The average power for condensation is less than 90 nW, which corresponds to peak power ~4 orders of magnitude higher. The dynamic condensate is far from thermal equilibrium, and its temperature is not well-defined. Nevertheless, the temperature of the semiconductor lattice can be controlled, and high lattice temperature has been shown previously to cause condensation deterioration in quasi-equilibrium systems due to phonon scattering [26]. Our experimental results show that at higher lattice temperature, higher pump intensities are required to reach a given coherence level [Fig. 3(b)] due to line broadening by phonons. Increasing the lattice temperature from 10 K to 50 K requires a ten-fold increase in pump intensity for condensation onset, comparable to recently reported results for non-resonantly generated polariton condensates [27].

Lastly, we have used the dynamics of macroscopic coherence accessible in our experiments to demonstrate the effect of the polariton interactions on the interference between two condensates. After the excitation pulse, the energy of the condensate Ψ is blue-shifted due to the mean-field interactions by $g|\Psi|^2$, an energy shift which increases with increasing pump intensity $I = P/A$, with P – pump power, and A – excitation spot area. This shift was demonstrated previously in spectral measurements [3,8,9]. In our time-dependent interference experiments, the first condensate will thus be blue-shifted, which will alter its phase relative to the second condensate generated at a later time. This phase shift $\Delta\varphi$ increases with the blue shift $g|\Psi|^2(t,I)$ and the delay time Δt:

$$\Delta\varphi = \int_0^{\Delta t} g|\Psi|^2(t,I)dt. \tag{5}$$

Therefore for constant delay time Δt, increasing the pump intensity I results in a larger phase difference between the two interfering condensates, visible as a spatial shift in the interference pattern.

We observed this nonlinear phase shift in our interference experiments [Fig. 4]. At a delay time of Δt = 6 ps, increasing I while keeping all other parameters constant results in a shift of the interference fringes with nearly linear dependence on I [Fig. 4(a)]. At a longer Δt = 16 ps, a larger shift of the interference pattern is observed due to a larger phase accumulation $\Delta\varphi$ = 6 ps [Fig. 4(b)]. The phase shift dependence is in good agreement with our calculations [Fig. 4(c)]. The demonstration of the nonlinear phase shift shown on Fig. 4, requires a long coherence time because the longer the interference can be observed – the larger the observed phase shift. The UP branch has a much shorter coherence time (~3ps) so no nonlinear phase shift could be clearly observed. From a nonlinear optics perspective, this phase shift represents an extremely strong nonlinear process. The observed phase shift here is on the scale of 10^{-4} rad/photon – two orders of magnitude larger than the recently reported results on cold-atom nonlinearities using electromagnetically-induced transparency [28]. Such nonlinearities are at the forefront of atomic physics research aimed at quantum nondemolition measurements and quantum computing [29]. In cold-atom systems, intensity-dependent phase shifts can be obtained for nearly-resonant transitions, but the maximum shift is limited by the atom density. In polariton condensates, the large nonlinearity stems from the inherent light-matter dressed states in the system. This optical nonlinearity is fundamentally different

#224691 - $15.00 USD Received 9 Oct 2014; revised 18 Nov 2014; accepted 19 Nov 2014; published 1 Dec 2014

because it is based on the strong Coulomb interaction between charged particles in the dressed states, in contrast to high-order multi-photon transitions in conventional nonlinear optics.

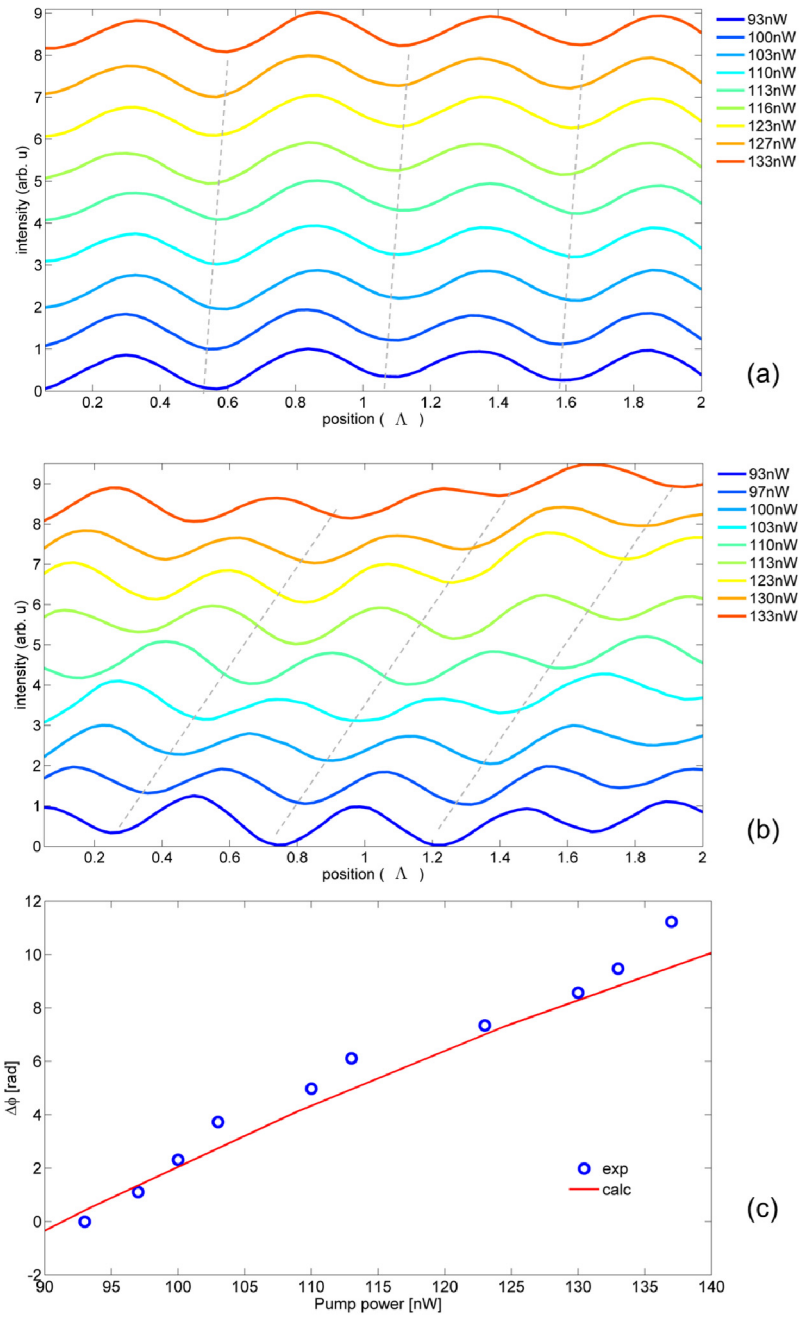

Fig. 4. Nonlinear phase shift measurements (a) Interference pattern shift with increasing pump power at Δt = 6 ps delay. The curves are horizontal slices of interference patterns with high-frequency noise filtered out. The curves are shifted vertically on the figure for clarity. The dashed lines are a guide to the eye following the fringe pattern minima, with $\Lambda = 2\pi/k_{\|}$. (b) Interference pattern shift with increasing pump power at Δt = 16 ps delay. (c) Nonlinear phase shift vs. pump power at Δt = 16 ps delay. The solid red line is the calculated dependence.

#224691 - $15.00 USD Received 9 Oct 2014; revised 18 Nov 2014; accepted 19 Nov 2014; published 1 Dec 2014

3. Conclusions

In conclusion, we have demonstrated coherence between quantum condensates generated by resonant polariton injection at different times. The coherence time is more than an order of magnitude longer than that defined by the initial injected bandwidth and the polariton dephasing time. The observed coherence follows the density dependence of condensation, despite being independent of the mass of the particles. We have shown that polariton-polariton interaction in the condensates results in a large nonlinear phase shift. Our results shed new light on the dynamics of coherence in matter, allowing the study of the ultrafast behavior of nonequilibrium condensates, and the development of new devices for future technologies.

#224691 - $15.00 USD Received 9 Oct 2014; revised 18 Nov 2014; accepted 19 Nov 2014; published 1 Dec 2014